Stochastic Modelling of Randomly Oriented Tapes Thermoplastic Composites in Net-Shaped Specimens

Gülmez, D.E.; Sinke, J.; Dransfeld, C.A.

Publication date
2022

Document Version
Final published version

Published in
Proceedings of the 20th European Conference on Composite Materials: Composites Meet Sustainability

ECCM 20

26-30 JUNE 2022

LAUSANNE SWITZERLAND

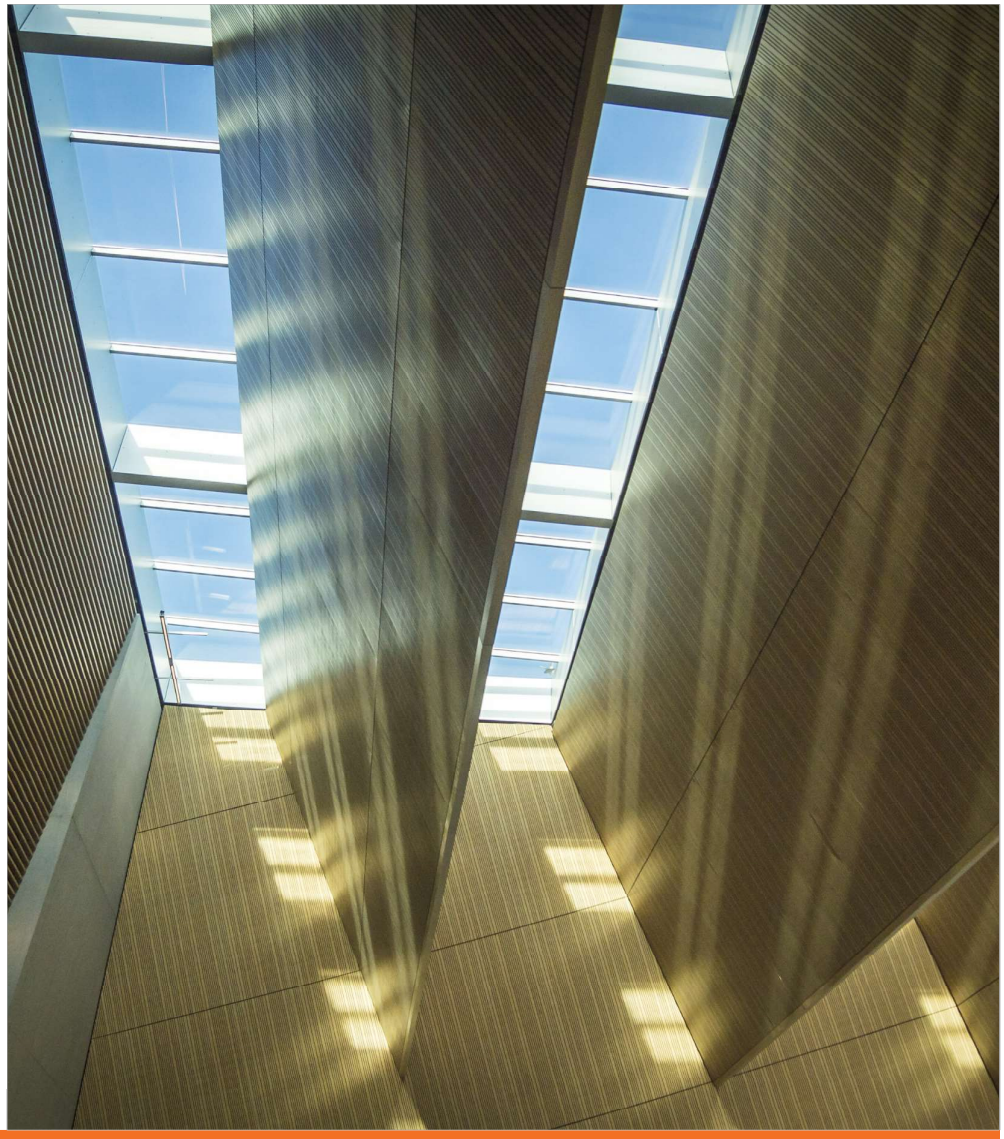

Proceedings of the 20th European Conference on Composite Materials

COMPOSITES MEET SUSTAINABILITY

Vol 4 – Modeling and Prediction

Editors : Anastasios P. Vassilopoulos, Véronique Michaud

Organized by :

EPFL

CCLAB Composite Construction Laboratory

Under the patronage of :

LPAC Laboratory for Processing of Advanced Composites

ESCM EUROPEAN SOCIETY FOR COMPOSITE MATERIALS

ECCM 20
26-30 JUNE 2022
LAUSANNE SWITZERLAND

EPFL CCLAB Composite Construction Laboratory LPAC Laboratory for Processing of Advanced Composites

Proceedings of the 20th European Conference on Composite Materials ECCM20 26-30 June 2022, EPFL Lausanne Switzerland

Edited By :

Prof. Anastasios P. Vassilopoulos, CCLab/EPFL
Prof. Véronique Michaud, LPAC/EPFL

Oragnized by:

Composite Construction Laboratory (CCLab)
Laboratory for Processing of Advanced Composites (LPAC)
Ecole Polytechnique Fédérale de Lausanne (EPFL)

ISBN: 978-2-9701614-0-0
DOI: http://dx.doi.org/10.5075/epfl-298799_978-2-9701614-0-0

Published by :

Composite Construction Laboratory (CCLab)
Ecole Polytechnique Fédérale de Lausanne (EPFL)
BP 2225 (Bâtiment BP), Station 16
1015, Lausanne, Switzerland

https://cclab.epfl.ch

Laboratory for Processing of Advanced Composites (LPAC)
Ecole Polytechnique Fédérale de Lausanne (EPFL)
MXG 139 (Bâtiment MXG), Station 12
1015, Lausanne, Switzerland

https://lpac.epfl.ch

Cover:

Swiss Tech Convention Center
© Edouard Venceslau - CompuWeb SA

Cover Design:

Composite Construction Laboratory (CCLab)
Ecole Polytechnique Fédérale de Lausanne (EPFL)
Lausanne, Switzerland

©2022 ECCM20/The publishers

Disclaimer:

STOCHASTIC MODELLING OF RANDOMLY ORIENTED TAPES THERMOPLASTIC COMPOSITES IN NET-SHAPED SPECIMENS

Deniz Ezgi Gulmez[a], Jos Sinke[a], Clemens Dransfeld[a]

a: Aerospace Manufacturing Technologies, Faculty of Aerospace Engineering, Delft University of Technology - D.E.Gulmez@tudelft.nl

Abstract: *Discontinuous tape composites have considerable attention due to their high formability and tailorable structures. Despite their advantages, this discontinuity leads to complex structures and makes it difficult to predict their mechanical properties. On the other hand, they have high orientational and dimensional sensitivity, which causes spatial variability and complexity in the structure to predict the mechanical properties. This spatial variability is also related to the mould cavity. A constitutive model was improved to explain the relationship between DT orientations and the mould cavity. According to the modelling technique, a random DT distribution was generated by Random Sequential Adsorption then, the Set Voronoi Tessellation was implemented to obtain DT layers. Afterwards, the Classical Laminate Theory and Finite Element Method were applied to compare the virtual net-shaped DT specimens. The results of both methods showed high stiffness at the edges of the specimens.*

Keywords: Discontinuous reinforcements; cavity edge effect; stiffness model; finite element modelling

1. Introduction

The tendency to use composite materials in the aircraft industry due to their lightweight and durable structures causes massive waste such as the out-of-date prepreg rolls, end of life aircraft structures and manufacturing cut-offs (1). Recycling, reuse and zero-waste manufacturing technologies have attracted considerable attention in reducing these wastes. Discontinuous thermoplastic composites minimize waste and offer recyclability. Besides their environmental advantages, they show high formability due to their discontinuous structure. This discontinuity helps to tailor mechanical properties such as increasing pseudo-ductility, which retards failure due to the shear lag between tapes (2).

On the other hand, they have high orientational and dimensional sensitivities, which cause spatial variability and complexity in the structure to predict the mechanical properties. This spatial variability is also related to the mould cavity. Experimental results of Discontinuous Tape (DT) composites have shown higher tensile modulus at the edges of the specimens than at the centre (3). Therefore, the mechanical properties of DT composites can be enhanced by using the edge effect of the mould. However, the relationship between mould cavity and tape orientation hasn't been well defined to understand the mechanical response of the DT composites and to improve the manufacturing routes.

The study aims to improve a modelling technique to explain the relationship between DT orientations and the mould cavity. The stiffness of the DT net-shaped specimens is calculated Classical Laminate Theory (CLT) and Finite Element Method (FEM) to evaluate and compare both results according to the width of the specimens.

  doi:10.5075/epfl-298799_978-2-9701614-0-0

2. Modelling

2.1 Randomization and Homogenization Algorithm

The Random Sequential Adsorbtion (RSA) algorithm (4) was modified by defining the distribution frame to generate a random distribution as seen in Fig. 1(a). According to this algorithm, random seed points and random angles between 0^0 and 179^0 in 2D were generated by considering a non-overlapped DT distribution inside the frame (Fig. 1(b)). The algorithm was continued for 4000 iterations to obtain a high filling ratio. DTs of 2.5 mm by 10 mm were placed in the virtual specimen dimensions of 150 by 60 mm in this study.

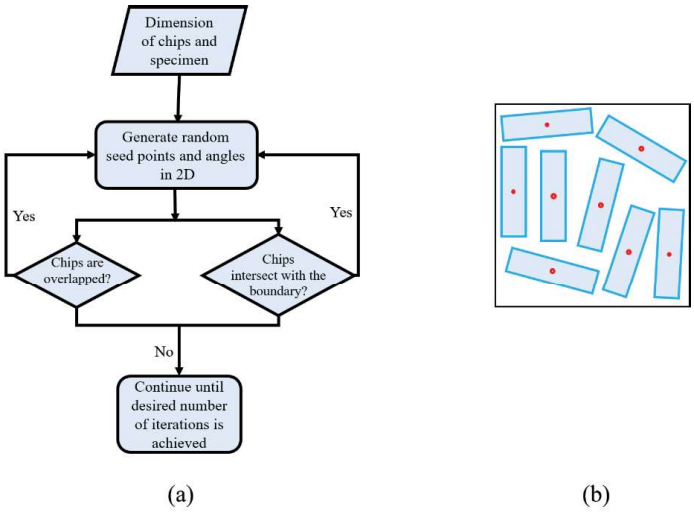

Figure 1. (a) Flowchart of the bounded-RSA algorithm and (b) the deposition result

After obtaining a DT distribution, the Set Voronoi tessellation (5) was implemented to define the local properties of each DTs layer and obtain full coverage of the DTs in the net-shaped frame. Elastic properties of the DTs were scaled according to the Set Voronoi Tessellation to implement the local variability to mechanical properties. the ratio between the tape area (A_t=l_t*w_t) and its cell area (A_c) was calculated (6). This ratio is called the local packing density (ϕ) as given in Eq. (1).

$$\phi = \frac{A_t}{A_c} \tag{1}$$

Elastic properties of AS4/PPS unidirectional (UD) prepreg tapes are scaled according to the local packing density (Table 1) and Eq. (2-5).

Table 1: Elastic Properties of UD AS4/PPS composite with a fibre volume ratio of 59% (7)

Longitudinal modulus, E_{11}	128 GPa
Transverse modulus, E_{22}	10.1 GPa
Shear modulus, G_{12}	5.7 GPa
Longitudinal Poisson's ratio, υ_{12}	0.37

$$E_{1i} = E_1 * \frac{\phi_i}{\phi_{avg}} \quad (2)$$

$$E_{2i} = E_2 * \frac{\phi_i}{\phi_{avg}} \quad (3)$$

$$G_{12i} = G_{12} * \frac{\phi_i}{\phi_{avg}} \quad (4)$$

$$\upsilon_{12i}, \upsilon_{21i} = \upsilon_{12}, \upsilon_{21} * \frac{\phi_i}{\phi_{avg}} \ (\upsilon_{12i}, \upsilon_{21i} \leq 0.49) \quad (5)$$

2.2 Laminate Analogy and Finite Element Model

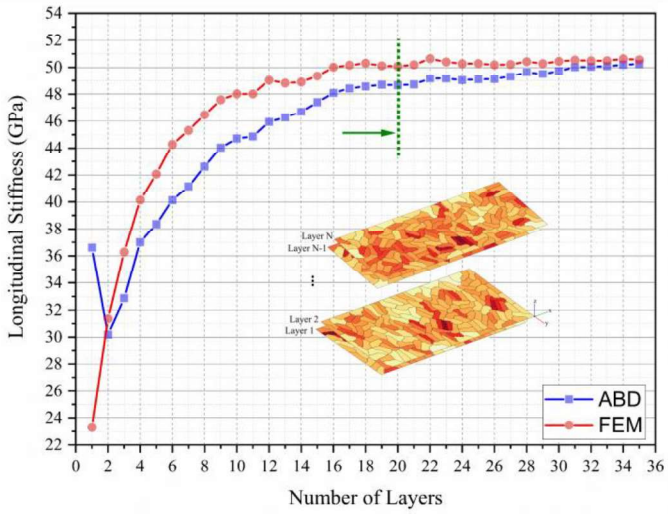

Figure 2. Convergence analysis for FEM and CLT models

A discretization process is necessary to implement CLT and FEM for each heterogeneous layer. The grid size is 1mm by 1mm. After the discretization of representative layers, the determination of the number of layers is another parameter to generate a representative specimen. As seen in Fig. 2, a convergence study was conducted to decide the number of layers for both CLT and FEM. In addition, the second-order orientation tensors in the two-dimension were calculated (8,9).

  doi:10.5075/epfl-298799_978-2-9701614-0-0

A, B, D matrices in CLT were calculated (Eq. (6-8)) by assuming each grid is an independent laminated composite:

$$A_{ij} = \sum_{k=1}^{n} Q_{ij}\,(z_k - z_{k-1}) \qquad i,j = 1,2,6 \tag{6}$$

$$B_{ij} = \frac{1}{2}\sum_{k=1}^{n} Q_{ij}\left(z_k^2 - z_{k-1}^2\right) \qquad i,j = 1,2,6 \tag{7}$$

$$D_{ij} = \frac{1}{3}\sum_{k=1}^{n} Q_{ij}\left(z_k^3 - z_{k-1}^3\right) \qquad i,j = 1,2,6 \tag{8}$$

The laminate compliance matrix (S), the longitudinal (E_x) and the transverse Modulus (E_y) were evaluated regarding (Eq. (9, 10)):

$$S = \begin{bmatrix} \alpha & \beta \\ \beta & \delta \end{bmatrix} = \begin{bmatrix} A & B \\ B & D \end{bmatrix}^{-1} \tag{9}$$

$$E_x = \frac{1}{t_s \alpha_{11}}\,, E_y = \frac{1}{t_s \alpha_{22}} \tag{10}$$

For Finite Element (FE) modelling of the virtual DT specimen, each partition assumed a FE and has an orientation angle after the discretization process. However, the elastic properties weren't scaled according to the tessellation approach to simplify the model. Tape angles are the only variable parameter for each FE. Therefore, an element size is 1 mm x 1 mm x 0.1 mm. Nodes are known and 8-node quad continuum shell elements (SC8R) can be obtained easily by using node data. Continuum shell elements have stacked through the thickness and one lamina is assigned for each SC8R element. A constant displacement is applied along the y-direction from one edge, encastre boundary condition is applied at the opposite edge, as seen in Fig. 3. ABAQUS/Standard (Implicit) input file is generated by using node and element data and defining boundary conditions and Hashin failure criteria (10) was implemented to evaluate the tensile response of the virtual specimens. Failure limits and fracture properties are given in Table 2. Viscous regularization factor was chosen at 0.00075.

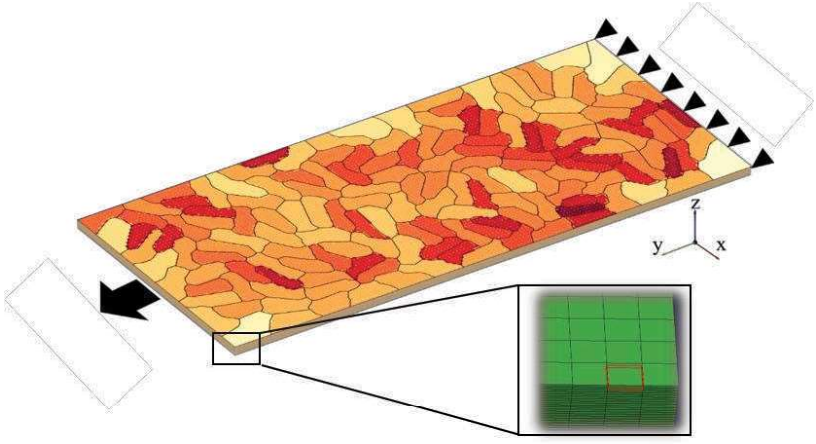

Figure 3. Boundary conditions of the representative virtual specimen

Table 2: Failure Limits and Fracture Properties of UD AS4/PPS composite (11,12)

Longitudinal tensile strength, X_t	2045 MPa
Longitudinal compressive strength, X_c	1117 MPa
Transverse tensile strength, Y_t	50 MPa
Transverse compressive strength, Y_t	90 MPa
Longitudinal shear strength, $S_{12}=S_{13}$	77 MPa
Fracture Energy, G_I	12.5 kJ/m^2
Fracture Energy, G_{II}	1.0 kJ/m^2

A net-shaped specimen was divided into regions as left, centre and right to understand the edge-orientations relationships as seen in Fig. 4. The size of the specimens was 60 mm by 150 mm. The width of the specimens at the edges was chosen as 8 mm considering the material loss due to the blade thickness for potential experimental validation. The width of the centre specimens was 40 mm. The length of all regional specimens was 150 mm.

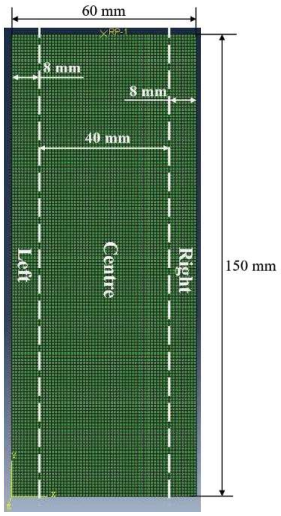

Figure 4. A representative virtual specimen, its regions and dimensions

3. Results and Discussion

Longitudinal Young Modulus distribution showed a high variability from 15 GPa to 95 GPa. However, the Young modulus in the longitudinal direction was the highest at the edges of the specimen, as given in Fig. 5 (a). When we look at Fig. 5 (b), matrix failure at 6.8 % global strain shows local variability due to the stiffness distribution all over the specimen. However, the result isn't related to the region of the specimen.

  doi:10.5075/epfl-298799_978-2-9701614-0-0 published under CC BY-NC 4.0 license

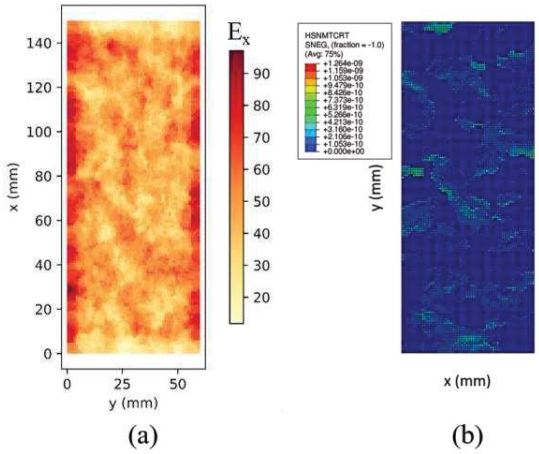

Figure 5. (a) Longitudinal stiffness and (b) Matrix failure (@6.8% strain) distribution in one virtual specimen

Longitudinal Young Modulus associated with orientation tensor in Fig. 6 (a). It was shown that the orientations of tapes were aligned length of the specimen. Thus, this alignment increases the stiffness at the edge of the net-shaped specimens. FEM results agreed with the high stiffness at the edges compared with the centre of the specimen as seen in Fig. 6 (b). In addition, matrix damage patterns were similar even though the specimens are cut according to the regions. However, their global mechanical response was variable. Specimens at the edges showed high tensile stress but low failure strain while low tensile stress and high failure strain were observed in the centre of the specimen.

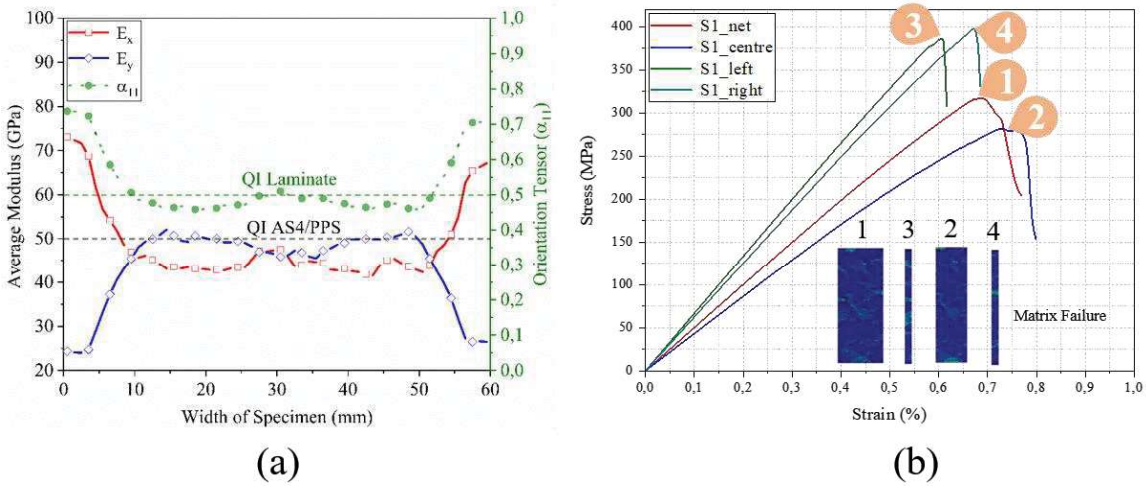

Figure 6. (a) Orientation tensor and elastic modulus through the width of one virtual specimen (b) Stress-Strain curve of one virtual specimen

Six virtual specimens were generated by using the modelling technique for both CLT and FEM evaluations to investigate the results statistically. Normalised stiffness results are given in Fig. 7. In general, both approaches showed high stiffness and a high range between minimum and maximum stiffness values at the edges. DTs are placed randomly and aligned at the edges

  doi:10.5075/epfl-298799_978-2-9701614-0-0 published under CC BY-NC 4.0 license

whereas DTs are highly random in the centre of the specimens. Thus, this range reduces in the centre for both CLT and FEM results.

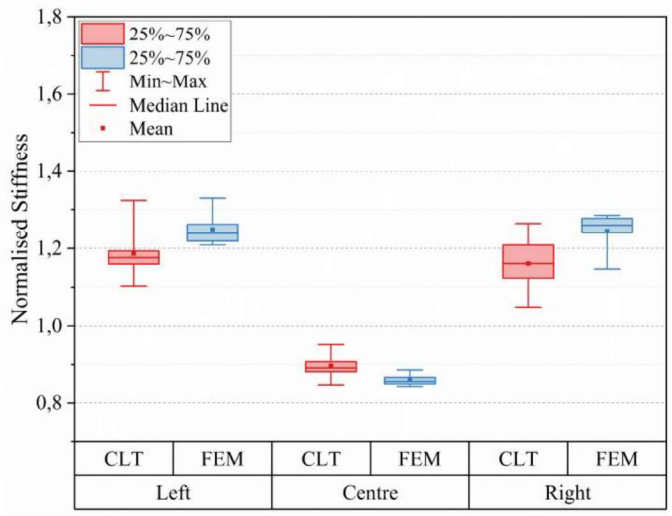

Figure 7. Comparison of normalized stiffness according to CLT and FEM

4. Conclusion

In this study, a modelling technique to predict the stiffness and strength of DT composites in net-shaped specimens was improved. The model generation starts with the RSA algorithm which is a defined frame of the distribution area to define the DT orientations. After that, a tessellation algorithm is implemented to obtain full coverage in the distribution area for discretization. According to the discretization, CLT and FEM are applied to evaluate the stiffness and strength of DT composites in net-shaped specimens. The results showed that stiffness at the edges of specimens is higher than in the centre of the specimens due to the high local alignment of DTs. This study demonstrates improving the mechanical properties of DT composites by controlling the DT orientations with the mould cavity.

Acknowledgements

We would like to thank Fraunhofer-Gesellschaft for their financial support.

5. References

1. Pimenta S, Pinho ST. Recycling carbon fibre reinforced polymers for structural applications: Technology review and market outlook. Waste Manag. 2011;31(2):378–92.

2. Czél G, Jalalvand M, Wisnom MR. Design and characterisation of advanced pseudo-ductile unidirectional thin-ply carbon/epoxy-glass/epoxy hybrid composites. Compos Struct [Internet]. 2016;143:362–70. Available from: http://dx.doi.org/10.1016/j.compstruct.2016.02.010

3. Tuttle M, Shifman T, Boursier B. Simplifying certification of discontinuous composite material forms for primary aircraft structures. In: International SAMPE Symposium and Exhibition (Proceedings). 2010.

4. Feder J. Random sequential adsorption. J Theor Biol. 1980;87(2):237–54.

5. Schallerab FM, Kapferac SC, Evansa ME, Hoffmanna MJF, Asted T, Saadatfare M, et al. Set Voronoi diagrams of 3D assemblies of aspherical particles. Philos Mag. 2013;93(31–33):3993–4017.

6. Völkel S, Huang K. Set Voronoi Tessellation for Particulate Systems in Two Dimensions. Springer Proc Phys. 2020;252(8):429–37.

7. Pappas G, Canal LP, Botsis J. Characterization of intralaminar mode I fracture of AS4/PPS composite using inverse identification and micromechanics. Compos Part A Appl Sci Manuf [Internet]. 2016;91:117–26. Available from: http://dx.doi.org/10.1016/j.compositesa.2016.09.018

8. Advani SG, creasy TS, Shuler SF. Chapter 8 Rheology of long fiber-reinforced composites in sheetforming. Compos Mater Ser. 1997;11(C):323–69.

9. Kravchenko SG, Pipes RB. Progressive Failure Analysis in Discontinuous Composite System of Prepreg Platelets with Stochastic Meso-Morphology. Sci Age Exp (SIMULIA User Meet. 2018;(June):1–14.

10. Hashin Z. Failure criteria for unidirectional fiber composites. J Appl Mech Trans ASME. 1980;47(2):329–34.

11. Pps- C. for Thermoplastic Composites. 2013.

12. Lapczyk I, Hurtado JA. Progressive damage modeling in fiber-reinforced materials. Compos Part A Appl Sci Manuf. 2007;38(11):2333–41.

